

Identification, evolution and functional characterization of two Zn
CDF-family transporters of the ectomycorrhizal fungus *Suillus luteus*

Peer-reviewed author version

RUYTINX, Joske; CONINX, Laura; NGUYEN, Hoai; SMISDOM, Nick; Morin, Emmanuelle; Kohler, Annegret; CUYPERS, Ann & COLPAERT, Jan (2017)
Identification, evolution and functional characterization of two Zn CDF-family transporters of the ectomycorrhizal fungus *Suillus luteus*. In: ENVIRONMENTAL MICROBIOLOGY REPORTS, 9(4), p. 419-427.

DOI: 10.1111/1758-2229.12551

Handle: <http://hdl.handle.net/1942/24371>

1 **Identification, evolution and functional characterization of two Zn CDF-family**
2 **transporters of the ectomycorrhizal fungus *Suillus luteus***

3

4 Joske Ruytinx^{1,*,+}, Laura Coninx^{1,*}, Hoai Nguyen¹, Nick Smisdom², Emmanuelle Morin³,
5 Annegret Kohler³, Ann Cuypers¹ and Jan V. Colpaert¹

6

7 ¹ Hasselt University, Centre for Environmental Sciences, Environmental Biology, Agoralaan
8 building D, 3590 Diepenbeek, Belgium

9 ² Hasselt University, Biomedical Research Institute, Agoralaan building C, 3590 Diepenbeek,
10 Belgium

11 ³ Institut National de la Recherche Agronomique, UMR1136 INRA-Université de Lorraine
12 Interactions Arbres/Microorganismes, Laboratoire d'Excellence ARBRE, 54280
13 Champenoux, France

14

15 * equally contributed to this work

16

17 ⁺ For correspondence:

18 joske.ruytinx@uhasselt.be; phone: +32 11 268377; fax: +32 11 268301

19

20 Running title: Identification and characterization of two Zn transporters

21

22 **Summary**

23 Two genes, *SlZnT1* and *SlZnT2*, encoding Cation Diffusion Facilitator (CDF) family
24 transporters were isolated from *Suillus luteus* mycelium by genome walking. Both gene
25 models are very similar and phylogenetic analysis indicates that they are most likely the result
26 of a recent gene duplication event. Comparative sequence analysis of the deduced proteins
27 predicts them to be Zn transporters. This function was confirmed by functional analysis in
28 yeast for *SlZnT1*. SlZnT1 was able to restore growth of the highly Zn sensitive yeast mutant
29 $\Delta zrc1$ and localized to the vacuolar membrane. Transformation of $\Delta zrc1$ yeast cells with
30 *SlZnT1* resulted in an increased accumulation of Zn compared to empty vector transformed
31 $\Delta zrc1$ yeast cells and equals Zn accumulation in wild type yeast cells. We were not able to
32 express functional SlZnT2 in yeast. In *S. luteus*, both *SlZnT* genes are constitutively expressed
33 whatever the external Zn concentrations. A labile Zn pool was detected in the vacuoles of *S.*
34 *luteus* free-living mycelium. Therefore we conclude that *SlZnT1* is indispensable for
35 maintenance of Zn homeostasis by transporting excess Zn into the vacuole.

36

37

38 **Keywords**

39 Zinc transporter, *Suillus luteus*, Zinc detoxification, Zinc storage, Cation Diffusion Facilitator

40 **Introduction**

41 Zinc (Zn) is an essential micronutrient as it is involved as co-factor, structural or signalling
42 element in a wide range of cellular processes (Eide, 2009). Nevertheless, it becomes toxic
43 when present in excess. The cellular Zn concentration of healthy, well-functioning cells
44 ranges from 0.1 - 0.5 mM. Most of the cellular Zn is bound to proteins and the labile/free
45 fraction is only in the nano to picomolar range (Eide, 2006; Simm *et al.*, 2007). To assure
46 cellular homeostasis in situations of Zn limitation as well as Zn surplus, all organisms require
47 a system to fine-tune Zn availability in the cell. This system is well studied in yeast and
48 mammals (Sekler *et al.*, 2007; North *et al.*, 2012) and is mainly relying on transporters. In all
49 eukaryotic cells, ZIP (Zrt-, Irt-like proteins) and CDF (cation diffusion facilitator) families of
50 transporters account for most of the Zn transport across membranes. ZIP transporters mediate
51 Zn transport towards the cytoplasm. They are involved in Zn uptake from the extracellular
52 space (environment) and remobilization from organelles (Kambe *et al.*, 2006). CDF
53 transporters remove Zn from the cytoplasm. Members of this family of transporters move Zn
54 to the extracellular space or into cellular compartments and therefore are involved in Zn
55 export and storage (Montanini *et al.*, 2007). However, ZIP and CDF family transporters are
56 not restricted to the transport of Zn. Both families enclose Zn, Fe and Mn transporters and
57 several of them are able to transport Cd in an unspecific way (Guerinot, 2000; Montanini *et*
58 *al.*, 2007). Substrate specificity of CDF family transporters can be predicted by phylogenetic
59 analysis that classifies CDF family transporters into three major groups, of which the
60 characterized members share the same metal specificity. Metal specificity of a newly
61 identified member can be inferred by its phylogenetic position in one of the three major
62 groups (Montanini *et al.*, 2007). Until now, metal specificity of ZIP transporters cannot be
63 predicted unambiguously from protein sequence only.

64 Mycorrhizal fungi are mutualists living in symbiosis with plant roots. They provide their host
65 plant with essential low-bioavailable nutrients as nitrogen and phosphorus in exchange for
66 photosynthesis-derived sugar (Smith & Read, 2008). Besides, this mutualism results in other
67 benefits for the host plant including protection from heavy metal stress. Mitigation of toxic
68 effects in plants by mycorrhizal fungi when grown in Zn-contaminated soils is well-
69 documented (Adriaenssen et al., 2004; Ferrol et al., 2016). Nevertheless, molecular
70 mechanisms of cellular Zn homeostasis in mycorrhizal fungi are not well-characterized and
71 their impact on plant nutrient balances is poorly understood. Detoxification of excess Zn in
72 mycorrhizal fungi includes storage in subcellular compartments. The ectomycorrhizal (ECM)
73 fungus *Suillus bovinus* stores excess Zn in vacuoles (Ruytinx et al., 2013); *Hebeloma*
74 *cylindrosporum*, another ECM fungus in ER-derived vesicles (Blaudez & Chalot, 2011). In *H.*
75 *cylindrosporum* a CDF family transporter HcZnT1, localized at the ER-membrane, is most
76 likely involved in the transport of cytoplasmic Zn towards the ER. A similar transporter was
77 characterized in the ericoid mycorrhizal (ERM) fungus *Oidiodendron maius* (Khouja et al.,
78 2013). RaCDF1 of *Russula atropurpurea* (ECM) clusters in phylogenetic analysis close to
79 HcZnT1 and OmZnT1, confers Zn tolerance to Zn sensitive yeast mutants but localizes on the
80 tonoplast and is likely involved in vacuolar Zn storage. A second transporter of the same
81 family, RaCDF2 was identified in this Zn-accumulating ectomycorrhizal fungus. RaCDF2 is
82 closely related to Mn transporting CDF's, localizes to the plasma membrane when
83 heterologous expressed in yeast, does not confer Mn tolerance to Mn sensitive yeast mutants
84 and likely acts as a bidirectional transporter of Zn, Cd and Co (Sacky et al., 2016). In
85 arbuscular mycorrhizal (AM) fungi *GintZnT1* of *Rhizophagus intraradices* was identified and
86 predicted to be a vacuolar Zn transporter of the CDF-family (Gonzalez-Guerrero et al., 2005).
87 Here we localize the labile Zn pool of *S. luteus* and report the functional characterization of
88 two CDF-family transporters. *S. luteus* is a cosmopolitan ectomycorrhizal fungus, associated

89 with pine trees. In particular, in primary successions of pines this species is abundant and
90 involved in seedling establishment (Hayward et al., 2015). On severely metal-contaminated
91 sites, Zn-tolerant *S. luteus* populations evolved and protect their host tree effectively from Zn
92 toxicity (Adriaensen et al., 2004; Colpaert et al., 2011). The *Suillus-Pinus* association has a
93 high potential for use in bio-stabilisation and restoration of metal-disturbed sites. However,
94 fundamental knowledge on the molecular mechanisms involved in metal homeostasis in the
95 plant and fungal partner is required to select most suited ecotypes and to fully exploit this
96 potential.

97 **Results and discussion**

98 **Localization of labile Zn pool in *S. luteus***

99 All fungi store excess Zn in a specific organelle where it is no longer able to harm the cell and
100 from where it can be remobilised in case of deficiency. For most fungi the vacuole is the main
101 site for Zn storage (Gonzalez-Guerrero *et al.*, 2008; Ott *et al.*, 2002; Simm *et al.*, 2007). On
102 the other hand, some fungi have special ER related vesicles (or zincosomes) for Zn storage
103 (Clemens *et al.*, 2002; Blaudez & Chalot 2011). Subcellular labeling of Zn in *S. luteus*
104 mycelium was performed with a fluorescent marker for free Zn^{2+} , FluoZin3 (Molecular
105 Probes, Invitrogen), which is able to detect free Zn^{2+} in the 1-100 nM range. A fluorescence
106 pattern, clearly indicating vacuoles, was observed (Fig. 1). Hyphae containing vacuoles with
107 labile Zn were distributed all over the mycelium (Fig. 1 a-c). External Zn concentration did
108 not change the observed fluorescence pattern, only intensity of the fluorescence changed. *S.*
109 *luteus* clearly stores Zn into the vacuole. No other accumulation pattern was detected despite
110 of different external Zn concentrations. Therefore vacuolar Zn storage is expected to be one of
111 the mechanisms to detoxify Zn and to maintain homeostasis in case of excess Zn in *S. luteus*.

112 **Identification and evolutionary origin of two *S. luteus* transporters of the CDF family**

113 CDF family transporters are often involved in Zn storage in vacuoles or ER related vesicles in
114 fungi. These transporters are key elements of the Zn homeostatic network of eukaryotes
115 (Montanini *et al.*, 2007; Kambe *et al.*, 2008; Gustin *et al.*, 2011). By removing Zn from the
116 cytosol they are particularly important in the prevention from Zn toxicity (Gaither & Eide,
117 2001). Using a genome walking approach targeting vacuolar Zn transporters of the CDF
118 family we picked up two *S. luteus* gene fragments. Further analysis by genome walking and
119 RACE protocols revealed that those fragments belong to the genes encoding proteins with
120 protein ID 807028 and 814105 in the JGI *S. luteus* genome database. The genes were named
121 *SlZnT1* and *SlZnT2* and both gene models are very alike (Supplemental figure S1). They
122 consist of 9 exons interspersed with introns of +/- 50 nucleotides. *In silico* translations of full
123 length cDNA's (1623 and 1516 bp) identified open reading frames of 1320 and 1362 bp
124 encoding a 440 and 453 amino acid-long polypeptide respectively (Fig. 2). A high percentage
125 of sequence identity (85%) between both predicted proteins is observed. The predicted
126 proteins show sequence and structural features typical of CDF family transporters.

127 CDF transporters are characterized by six transmembrane domains and a histidine rich motif
128 (HX)_n in the cytosolic loop between transmembrane helices IV and V. For most proteins of
129 this transporter family the histidine rich motif is located directly after helix IV and contains
130 three to six HX repeats (Gaither & Eide, 2001). The topology prediction program TMHMM
131 predicted 6 transmembrane domains for both deduced *S. luteus* proteins. The deduced proteins
132 are very similar but show a considerable level of sequence diversification in the cytosolic loop
133 between helix IV and V (Fig. 2). *SlZnT1* is with its predicted six transmembrane domains and
134 (HX)₃ domain a typical CDF family member. *SlZnT2* is somewhat aberrant since the normal
135 (HX)_n motif shows seven repeats and an extra, second (HX)_n motif (n=5) is present just before
136 helix V. The exact function of the (HX)_n motif is unclear but it is expected to have a role in
137 metal recruitment (Gaither & Eide, 2001). In plants the histidine-rich loop is hypothesized to

138 play a role as a Zn chaperone to determine the identity of the transported ions (Podar et al.,
139 2012). The atypical sequence of SlZnT2 with the presence of an additional (HX)_n motif might
140 therefore have some implications for metal selectivity and specificity. However, Lin *et al.*
141 (2009) showed that metal specificity is determined by a cooperation between transmembrane
142 domain II and V. Several single amino acid substitutions within transmembrane helices II and
143 V of the *S. cerevisiae* vacuolar Zn transporter *ZRC1* resulted in an Fe and Mn transporting
144 protein. Some of these proteins created by site directed mutagenesis retained the ability to
145 transport Zn, others not (Lin *et al.*, 2008; Lin *et al.*, 2009). In particular the amino acid
146 located four residues before the highly conserved aspartate (D) in transmembrane domain II
147 and V is very important in metal selectivity (Montanini *et al.*, 2007). Both identified *S. luteus*
148 transporters have a HXXXD motif in transmembrane helices II and V, a feature specific for
149 the group of Zn transporting CDFs (Fig. 2).

150 Comparisons with the NCBI nr protein sequences (BLASTx) or fungal protein models at jgi
151 MycoCosm resulted in the same hits for SlZnT1 and SlZnT2. However, ranking of the hits is
152 different. Previously characterized CDF family transporters with the highest sequence identity
153 are the RaCDF1 protein of *Russula atropurpurea* (53%) and the GintZnT1 protein of
154 *Rhizophagus intraradices* (44%) for SlZnT1 and SlZnT2, respectively. All hits are protein
155 models corresponding to CDF family transporters. Remarkable is that only species from the
156 suborder *Suillineae* and *Coniophora puteana* occur twice in the list of BLASTx hits. To
157 elucidate the origin and relationship of SlZnT1 and SlZnT2 a neighbour-joining (NJ) tree was
158 built using previously characterized fungal CDF family transporters and BLASTx hits. In this
159 tree (Fig. 3) both SlZnT1 and SlZnT2 cluster to the Zrc1/Cot1-like Zn-CDFs (Montanini *et al.*
160 2007). Within the cluster of Zrc1/Cot1-like CDFs, SlZnT1 clusters with the majority of the
161 BLASTx hits while SlZnT2 divergates earlier and groups in a cluster that only contains
162 sequences of species that had two BLASTx hits. Reconciliation of the tree with an ITS

163 phylogeny of the considered taxa supports a gene duplication in the common ancestor of
164 Suillineae and the Coniophora/Serpula clade (supplemental figure S2). Gene expansion and
165 loss are common events in fungal genome evolution and may result in phenotypic alterations
166 (Floudas *et al.*, 2012, Kohler *et al.*, 2015). Interestingly, *S. luteus* and some other species
167 within the Suillineae clade are known to evolve Zn-tolerant phenotypes on severely metal-
168 contaminated soils (Colpaert *et al.*, 2004). Members of the SlZnT2 cluster could therefore be
169 candidate genes to study in adaptive Zn tolerance of Suilloid fungi. Five additional *S. luteus*
170 genes predicted to encode CDF transporters were identified and cluster within different
171 clusters of the phylogenetic tree (Fig.3 and Supplemental figure S3).

172 **Functional characterization of *SlZnT1* in yeast**

173 *SlZnT1* was expressed in yeast to confirm the functionality predicted by comparative
174 sequence analysis. Heterologous expression in the eukaryotic model system *S. cerevisiae* is a
175 common strategy to get insight into gene function (Osborn & Miller, 2007; Mokdad-Gargouri
176 *et al.*, 2012). By comparative gene analysis, *SlZnT1* is predicted to encode a vacuolar Zn
177 transporter. *SlZnT1* gene product was able to partly restore growth of $\Delta zrc1$, a yeast mutant
178 defective in vacuolar Zn storage and highly sensitive for Zn, on Zn enriched medium (Fig. 4).
179 The highly sensitive phenotype of $\Delta cot1$ (defective vacuolar CDF transporter) on cobalt (Co)
180 containing medium could not be restored by the identified *S. luteus* gene product. Also, the
181 defective vacuolar ATP (adenosine triphosphate) binding cassette of $\Delta ycf1$ (Cd sensitive)
182 yeast and the defective golgi P-type ATPase of $\Delta pmr1$ (Mn sensitive) yeast could not be
183 complemented by SlZnT1 (Supplementary figure S4).

184 To better understand the role of *SlZnT1* in Zn homeostasis the cellular metal content of wild
185 type yeast (+ empty vector (EV)), $\Delta zrc1$ (+EV) and $\Delta zrc1$ carrying *SlZnT1* was determined
186 after exposure to Zn. All yeast cultures showed an increased Zn content after growing in Zn
187 enriched medium (Supplemental fig. S6). Wild type yeast and $\Delta zrc1$ yeast containing *SlZnT1*

188 accumulated a comparable amount of Zn. This amount is significantly higher than the amount
189 measured in $\Delta zrc1$. No significant differences in Fe and Mn content were observed among the
190 yeast mutants when exposed to Zn (Supplementary figure S7), indicating the Zn specificity of
191 the transporter. Translational fusion of *SlZnT1* to GFP confirmed its vacuolar localization in
192 yeast (Fig. 5). Yeast cells containing the *SlZnT1::EGFP* fusion construct showed a bright
193 green GFP fluorescent ring at the level of the vacuolar membrane (Fig. 5a-d). Clear co-
194 localisation of the GFP fluorescence with the red fluorescence of the tonoplast specific
195 staining FM4-64 was observed for the *SlZnT1::EGFP* fusion construct.

196 All together our observations support a ZRC1-like function for *SlZnT1*. ZRC1 is involved in
197 vacuolar Zn storage and largely determines yeast's ability to detoxify excess Zn (Kamizono et
198 al., 1989). Most likely, *SlZnT1* has a role in cellular Zn homeostasis in *S. luteus* by
199 transporting excess Zn towards the vacuolar stock.

200 **Functional characterization of *SlZnT2* in yeast**

201 Although *SlZnT1* and *SlZnT2* are very similar, we were not able to express functional *SlZnT2*
202 in *S. cerevisiae*. None of metal sensitive phenotypes of the tested yeast mutants defective in
203 metal transport could be complemented by expression of *SlZnT2* (Fig. 4 and supplemental
204 figure S4). Though, the gene is clearly expressed since *SlZnT2* transcript could be detected in
205 the transformed yeast cells by PCR (Supplementary figure S5). Translational fusion to GFP
206 resulted in accumulation of GFP inside the vacuole (Fig. 5). Fusion of the EGFP protein to
207 *SlZnT2* resulted in a green fluorescent vacuolar content when expressed in yeast for both N-
208 terminal and C-terminal fusion. Figure 5 (e-g) shows that EGFP fluorescence is nicely
209 surrounded by FM4-64 fluorescence. Zn content of $\Delta zrc1$ containing *SlZnT2* was similar to
210 that of $\Delta zrc1$ containing the empty vector and is significantly lower than in WT yeast cells
211 exposed to the same external Zn concentration (Supplemental fig. S6).

212 Heterologous expression is a powerful way to study gene function but has some limitations
213 because of differences in e.g. codon usage, posttranscriptional regulation, posttranslational
214 modifications and protein targeting signals (Yin *et al.*, 2007; Mattanovich *et al.*, 2012). These
215 differences might be at the basis of the non-functioning of *SlZnT2* in yeast. The functional
216 characterization of the *R. intraradices* CDF transporter *GintZnT1* in yeast resulted in similar
217 problems. Although, *GintZnT1* could be detected by western blotting in transformed cells, it
218 was not able to complement any metal sensitive yeast mutants. This transporter could not be
219 affiliated to a specific membrane; the expressed protein seemed to accumulate all over the
220 cytoplasm (Gonzalez-Guerrero *et al.*, 2005). However, the exact reason of non-functioning is
221 probably different for both proteins since they accumulate in different cellular compartments
222 in yeast. Regulation of posttranslational modifications and protein targeting are only little
223 explored in mycorrhizal fungi and deserve further attention.

224 ***SlZnT1* and *SlZnT2* gene expression in *S. luteus***

225 Gene expression levels of *SlZnT1* and *SlZnT2* were determined in *S. luteus* after 48h exposure
226 to different concentrations of Zn, including concentrations inducing cellular Zn deficiency
227 and toxicity. Figure 6a and 6b show that both *SlZnT1* and *SlZnT2* expression were
228 constitutive. Neither exposure to excess Zn, nor limiting Zn changed the expression level of
229 the transporters when compared to the control condition (20 μ M Zn). On average *SlZnT1* and
230 *SlZnT2* expression level differ by at least a factor five, with *SlZnT2* showing the lowest
231 transcript abundance (Fig. 6a and 6b). Insensitivity of gene expression for high external Zn
232 concentrations was demonstrated previously for the Zn CDF transporter *ZRC1* of *S. cerevisiae*
233 (MacDiarmid *et al.*, 2003) and *HcZnT1* of *Hebeloma cylindrosporum* (Blaudez & Chalot,
234 2011). However, in *R. intraradices* gene expression of the *SlZnT* homologous gene *GintZnT1*
235 is transiently induced by elevated external Zn concentrations (Gonzalez-Guerrero *et al.*,
236 2005). *S. cerevisiae* cells show a proactive strategy of homeostatic regulation of free cellular

237 Zn content by an induction of *ZRC1* gene expression in Zn limited cells (MacDiarmid *et al.*,
238 2003). Being proactive guarantees a rapid resistance in case of depletion. In *S. luteus* no
239 change in *SlZnT* gene expression level was detected after growth without Zn for 48h (Fig. 6).
240 This might imply that both *SlZnT*'s are not regulated proactive neither reactive by external Zn
241 concentration at the transcriptional level.

242 **Conclusion**

243 *SlZnT1* probably has a key role in vacuolar Zn storage in *S. luteus* considering the results
244 obtained by heterologous expression in yeast. Based on the phylogenetic analysis it is likely
245 that *SlZnT2* is involved in vacuolar Zn storage as well. However, redundancy caused by gene
246 duplication might lead to diversification and neo-functionalization (Assis & Bachtrog, 2013).
247 Subcellular targeting of *SlZnT2* is unclear and vacuolar localisation was not confirmed. This
248 protein might have evolved to transport Zn out of the cell by localisation to the plasma
249 membrane or ER. Since we could never observe a zincosomes related accumulation pattern in
250 *S. luteus*, a role for *SlZnT2* in Zn detoxification by storage or secretion via zincosomes is
251 rather unlikely unless Zn is tightly bound to a chelator, preventing its detection by the
252 fluorescent marker. Also, Zn specificity of *SlZnT2* was not confirmed and comparative
253 sequence analyses are not always conclusive. RaCDF2 of *Russula atropurpurea* is a Zn
254 exporting plasma membrane transporter nested within a cluster of Mn transporters and
255 without the Zn-specific HXXXD motif in transmembrane helices II and V (Sacky *et al.*,
256 2016). CDFs are conserved proteins and this kind of changes in metal specificity seem rather
257 exceptional since all other previously characterized CDFs of Bacteria, Plants and Animals
258 cluster in phylogenetic trees according to the metal they are transporting (Montanini *et al.*,
259 2007; Cubillas *et al.*, 2013). A role of *SlZnT2* in Zn transport and homeostasis of *S. luteus* is
260 likely. Other *S. luteus* genes are predicted to function in Fe and Mn transport. Five additional
261 CDF-encoding genes were identified in the *S. luteus* genome (Fig. 3 and Supplemental figure

262 S3). These genes need to be further characterized to confirm their putative role and
263 understand their contribution in Zn, Fe and Mn homeostasis of *S. luteus*.

264 **Acknowledgements**

265 We greatly acknowledge Carine Put, Pieter Ceysens and Bram Vanhumbeeck for technical
266 assistance. This research was financially supported by the Research Foundation – Flanders
267 (FWO-project G.0925.10 and G.0792.13) and a Methusalem project (08M03).

268 **Competing interest**

269 The authors declare that they have no competing interest

270 **References**

- 271 Adriaensen, K., van der Lelie, D., Van Laere, A., Vangronsveld, J., Colpaert, J.V. (2004) A
272 zinc-adapted fungus protects pines from zinc stress. *New Phytol* 161(2): 549-555.
- 273 Assis, R., Bachtrog, D. (2013) Neofunctionalization of young duplicate genes in *Drosophila*.
274 *Proc Natl Acad Sci USA* 110: 17409-17414.
- 275 Blaudez, D., Chalot, M. (2011) Characterization of the ER-located zinc transporter ZnT1 and
276 identification of a vesicular zinc storage compartment in *Hebeloma cylindrosporium*.
277 *Fungal Genet Biol* 48: 496-503.
- 278 Clemens, S., Bloss, T., Vess, C., Neumann, D., Nies, D.H., Zur Nieden, U. (2002) A
279 transporter in the endoplasmic reticulum of *Schizosaccharomyces pombe* cells
280 mediates zinc storage and differentially affects transition metal tolerance. *J Biol Chem*
281 277: 18215-18221.
- 282 Colpaert, J.V., Muller, L.A.H., Lambaerts, M., Adriaensen, K., Vangronsveld, J. (2004)
283 Evolutionary adaptation to Zn toxicity in populations of Suilloid fungi. *New Phytol*
284 162: 546-559.
- 285 Colpaert, J.V., Wevers, J.H.L., Krznic, E., Adriaensen, K. (2011) How metal-tolerant
286 ecotypes of ectomycorrhizal fungi protect plants from heavy metal pollution. *Annals*
287 *of Forest Science* 68:17–24.
- 288 Cubillas, C., Vimiesa, P., Tabche, M.L., Garcia-de los Santos, A. (2013) Phylogenomic
289 analysis of cation diffusion facilitator proteins uncovers Ni²⁺/Co²⁺ transporters.
290 *Metallomics* 5: 1634-1643.
- 291 Eide, D.J. (2006) Zinc transporters and the cellular trafficking of zinc. *Biochim Biophys Acta*
292 1763: 711-722.
- 293 Eide, D.J. (2009) Homeostatic and adaptive responses to zinc deficiency in *Saccharomyces*
294 *cerevisiae*. *J Biol Chem* 284: 18565-18569.

295 Ferrol, N., Tamayo, E., Vargas, P. (2016) The heavy metal paradox in arbuscular
296 mycorrhizas: from mechanisms to biotechnological applications. *J Exp Bot* 67:6253-
297 6265.

298 Floudas, D., Binder, M., Riley, R., Barry, K., Blanchette, R.A., Henrissat, B., Martinez, A.T.,
299 Otiillar, R., Spatafora, J.W., Yadav, J.S. *et al.* 2012. The Paleozoic origin of enzymatic
300 lignin decomposition reconstructed from 31 fungal genomes. *Science* 336: 1715-1719.

301 Gaither, L.A., Eide, D.J. (2001) Eukaryotic zinc transporters and their regulation. *Biometals*
302 14(3-4): 251-270.

303 Gonzalez-Guerrero, M., Azcon-Aguilar, C., Mooney, M., Valderas, A., MacDiarmid, C.W.,
304 Eide, D.J., Ferrol, N. (2005). Characterization of a *Glomus intraradices* gene encoding
305 a putative Zn transporter of the cation diffusion facilitator family. *Fungal Genet Biol*
306 42: 130-140.

307 Gonzalez-Guerrero, M., Melville, L.H., Ferrol, N., Lott, J.N.A., Azcon-Aguilar, C., Peterson,
308 R.L. (2008) Ultrastructural localization of heavy metals in the extraradical mycelium
309 and spores of the arbuscular mycorrhizal fungus *Glomus intraradices*. *Can J Microbiol*
310 54: 103-110.

311 Guerinot, M.L. (2000). The ZIP family of metal transporters. *Biochim Biophys Acta* 1465:
312 190-198.

313 Gustin, J., Zanis, M., Salt, D. (2011) Structure and evolution of the plant cation diffusion
314 facilitator family of ion transporters. *BMC Evol Biol* 11: 76.

315 Hayward, J., Horton, T.R., Pauchard, A., Nuñez, M.A. (2015) A single ectomycorrhizal
316 fungal species can enable a *Pinus* invasion. *Ecology* 96: 1438-1444.

317 Kambe, T., Suzuki, T., Nagao, M., Yamaguchi-Iwai, Y. (2006) Sequence similarity and
318 functional relationship among eukaryotic ZIP and CDF transporters. *Genomic*
319 *Proteomic Bioinformatic* 4(1): 1-9.

320 Kambe, T., Weaver, B., Andrews, S. (2008) The genetics of essential metal homeostasis
321 during development. *Genesis* 46: 214-228.

322 Kamizono, A., Nishizawa, M., Teranishi, Y., Murata, K., Kimura, A. (1989) Identification of
323 a gene conferring resistance to zinc and cadmium ions in the yeast *Saccharomyces*
324 *cerevisiae*. *Mol Gen Genet* 219: 161-167.

325 Khouja, H.R., Abba, S., Lacercat-Didier, L., Daghino, S., Doillon D., Richaud, P., Martino,
326 E., Vallino M., Perotto S., Chalot, M., Blaudez D. (2013) OmZnT1 and OmFET, two
327 metal transporters from the metal-tolerant strain Zn of the ericoid mycorrhizal fungus
328 *Oidiodendron maius*, confer zinc tolerance in yeast. *Fungal Genetics and Biology*
329 52:53-64.

330 Kohler, A., Kuo, A., Nagy, L.G., Morin, E., Barry, K.W., Buscot, F. et al. (2015) Convergent
331 losses of decay mechanisms and rapid turnover of symbiosis genes in mycorrhizal
332 mutualists. *Nat Genet* 47: 410-415.

333 Lin, H., Kumanovics, A., Nelson, J.M., Warner, D.E., Ward, D.M., Kaplan, J. (2008). A
334 single amino acid change in yeast vacuolar metal transporters ZRC1 and COT1 alters
335 their substrate specificity. *J Biol Chem* 283: 33865-33873.

336 Lin, H., Burton, D., Li, L., Warner, D.E., Philips, J.D., Ward, D.M., Kaplan, J. (2009) Gain of
337 function mutants identify amino acids within transmembrane domains of the yeast
338 vacuolar transporter Zrc1 that determine metal specificity. *Biochem J* 422: 273-283.

339 MacDiarmid, C.W., Milanick, M.A., Eide, D.J. (2003) Induction of the ZRC1 metal tolerance
340 gene in zinc-limited yeast confers resistance to zinc shock. *J Biol Chem* 278: 15065-
341 15072.

342 Mattanovich, D., Branduardi, P., Dato, L., Gasser, B., Sauer, M., Porro, D. (2012)
343 Recombinant protein production in yeast. *Method Mol Biol* 824: 329-359.

344 Mokdad-Gargouri, R., Abdelmoula-Soussi, S., Hadiji-Abbès, N., Amor, I.Y., Borchani-
345 Chabchoub, I., Gargouri, A. (2012) Yeasts as a tool for heterologous gene expression.
346 Method Mol Biol 824: 359-370.

347 Montanini, B., Blaudez, D., Jeandroz, S., Sanders, D., Chalot, M. (2007) Phylogenetic and
348 functional analysis of the cation diffusion facilitator (CDF) family: improved signature
349 and prediction of substrate specificity. BMC Genomic 8: 107-122.

350 North, M., Steffen, J., Longuinov, A., Zimmerman, G., Vulpe, C., Eide, D. (2012) Genome-
351 wide functional profiling identifies genes and processes important for zinc limited
352 growth of *Saccharomyces cerevisiae*. PLOS Genet 8(6): e1002699.

353 Osborn, M.J., Miller, J.R. (2007) Rescuing yeast mutants with human genes. Brief Funct
354 Genomic Proteomic 6: 104-111.

355 Ott, T., Fritz, E., Polle, A., Schützendübel, A. (2002) Characterization of antioxidative
356 systems in the ectomycorrhiza-building basidiomycete *Paxillus involutus* (Bartsch) Fr.
357 and its reaction to cadmium. FEMS Microbiol Ecol 42: 359-366.

358 Podar, D., Scherer, J., Noordally, Z., Herzijk, P., Nies, D., Sanders, D. (2012) Metal
359 selectivity determinants in a family of transition metal transporters. J Biol Chem 287:
360 3185-3196.

361 Ruytinx, J., Nguyen, N., Van Hees, M., Op De Beeck, M., Vangronsveld, J., Carleer, R.,
362 Colpaert, J.V., Adriaensen, K. (2013) Zinc export results in adaptive zinc tolerance in
363 the ectomycorrhizal basidiomycete *Suillus bovinus*. Metallomics 5: 1225-1233

364 Säcký, J., Leonhardt, T., Kotrba P. (2016) Functional analysis of two genes coding for
365 distinct cation diffusion facilitators of the ectomycorrhizal Zn-accumulating fungus
366 *Russula atropurpurea*. Biometals 29:349–363.

367 Sekler, I., Sensi, S.L., Herschfinkel, M., Silverman, W.F. (2007) Mechanism and regulation
368 of cellular zinc transport. Mol Med 13(7-8): 337-343.

369 Simm, C., Lahner, B., Salt, D., LeFurgey, A., Ingram, P., Yandell, B., Eide, D.J. (2007)
370 *Saccharomyces cerevisiae* vacuole in zinc storage and intracellular zinc distribution.
371 Eukaryot Cell 6: 1166-1177.

372 Smith S.E., Read D.J. (2008) Mycorrhizal symbiosis (third edition). Academic Press.

373 Yin, J., Li, G., Ren, X., Herrler, G. (2007) Select what you need: a comparative evaluation of
374 the advantages and limitations of frequently used expression systems for foreign
375 genes. J Biotechnol 127: 335-347.

376

377 **Supplementary Table 1. Degenerative primers used in the genome walking protocol.**

name	sequence
DG1aS	GTNGCNGAYAGYTTYCAYATGCT
DG1bS	ATYGCNGAYTCATTYCAATG
DG2aS	CAMCGWGCRGARATTCTNGCNGC
DG2bS	AAMGNGCRGARATTTTRGGTGCT
DG3aS	CTTGCSCTNTGYNTCTCNAT
DG3bS	ATTGCCYTNTGYNTSTYNATT
DG4aAS	AGNASASCAYGCATR TTCAT
DG4bAS	AASACACCATGCATATATTYAA
DG5aAS	CCNACR TTNCCNAGRGCR TC
DG5bAS	RCCRATR TTRCCNAGAGCATC
DG6aAS	TCNAARTARTAYTTCCARCTCCA
DG6bAS	RTARTANYKCCAAGAATAKTCRGT

378 **Supplementary Table 2. Gene specific primers used in the different protocols.**

name	sequence	target	protocol
ZnT1L	GGCATCACGAAACCATGACTTCAT	ZnT1	walking/RACE/gene expression
ZnT1R	GGTACTCGGGTTGAATAGTACTAGAATGT	ZnT1	walking/RACE/gene expression
ZnT1a	TCGGAGGAGTCTTATGGTCG	ZnT1	walking/RACE
ZnT1b	TGCGGGGGCGTATAATGAGA	ZnT1	walking
ZnT1c	CCTGGAGTAAAGAAGCGCTCT	ZnT1	walking
ZnT1d	CCTGCAATGAGCTCAATGAAGAAGAAGAA	ZnT1	walking
ZnT1Ra	ACATTCTAGTACTATTCAACCCGAGTACC	ZnT1	walking/RACE
ZnT2L	CGACGGTAAGGTGGAAATAAAC	ZnT2	walking/RACE/gene expression
ZnT2R	TGGTGAGCCAGATGACAAGA	ZnT2	walking/RACE/gene expression
ZnT2a	CCATGCGAATGAGAGTGACCA	ZnT2	walking
ZnT2b	CCAGCCGTAGGAGTAACGA	ZnT2	walking
ZnT2c	GATGCGAGCTGAACGAGATAA	ZnT2	walking/RACE
ZnT2d	CGTCATTACATCTCCAGAACATTCCAT	ZnT2	walking

379

380 **Figure 1. Labile Zn pool, marked with FluoZin 3, in *S. luteus*.** (a-c) Overview of
381 peripheral hyphae of the mycelium; (d-f) detailed view of hyphae showing vacuoles. (a,d)
382 Differential interference contrast image, (b,e) green fluorescence of labile Zn bound to
383 FluoZin3, (c,f) merged image showing fluorescence in vacuoles. Scale bars: (a-c) 10 μm ;
384 5 μm .

385 **Figure 2. Alignment of SIZnT1 and SIZnT2 encoded proteins.** Residues are Rasmol
386 coloured. The six transmembrane domains predicted by topology prediction program
387 TMHMM are indicated by arrows; the histidine rich motifs (HX)_n between transmembrane
388 helix IV and V are indicated by braces. The Zn specific HXXXD domains are framed by a
389 dotted box.

390 **Figure 3. Neighbour-joining (NJ) tree of the Cation Diffusion Facilitator (CDF) family**
391 **proteins from selected fungi.** Sequences were aligned by the MAFFT algorithm. Bootstrap
392 values (1000 replicates) are indicated and branch lengths are proportional to phylogenetic
393 distances. Localization and substrate (metal) are indicated for functionally characterized
394 proteins. Mn and Fe clusters are collapsed. *S. luteus* sequences are framed, SIZnT1 and
395 SIZnT2 are indicated by an arrow. V = vacuole; ER = endoplasmic reticulum, G = Golgi
396 apparatus.

397 **Figure 4. Functional complementation of the Zn sensitive yeast mutant Δzrc1 .** Cultures of
398 wild type and mutant yeast were tenfold serial diluted and spotted on control and Zn-
399 supplemented SD medium. The wild type strain was transformed with the empty vector, the
400 mutant strain with either the empty vector or the vector containing *SIZnT1* or *SIZnT2*. The
401 experiment was carried out twice for three independent clones and pictures were taken after 4
402 days of growth.

403 **Figure 5. Localisation of SIZnT1:EGFP (a-d) and SIZnT2:EGFP (e-h) fusion proteins in**
404 **yeast.** (a,e) bright field image, (b,f) EGFP fusion protein, (c,g) FM4-64 vacuolar membrane

405 staining, (d, h) merged images. *SlZnT1*:GFP and FM4-64 tonoplast staining co-localize and
406 *SlZnT2*:GFP is detected inside the vacuole.

407 **Figure 6. Relative gene expression level of (a) *SlZnT1* and (b) *SlZnT2* in *S. luteus***
408 **mycelium after 48h exposure to different concentrations of Zn as measured by qPCR.**

409 Data are the average +/- SE of seven biological replicates. Both genes were constitutively
410 expressed, no significant differences as compared to the control were detected.

411 **Supplemental Figure S1. Gene model for the two newly identified *S. luteus* transporters,**
412 **(a) *SlZnT1* and (b) *SlZnT2*.** Untranslated regions (UTRs) are coloured green, exons red and
413 introns are represented by a line. Length (amount of nucleic acids) of each individual part is
414 indicated above (UTR and exon) or beneath (intron) the corresponding region.

415 **Supplemental Figure S2. Evolution of fungal CDF transporters of the *zrc1/cot1* cluster.**
416 Reconciled tree of the *zrc1/cot1* cluster of CDF transporters using a maximum likelihood ITS
417 phylogeny of selected fungal species supporting five independent gene duplication events
418 (indicated in red). Seven gene loss events were predicted (represented in grey). *SlZnT1* and
419 *SlZnT2* originate from a duplication event (indicated by an arrow) in the common ancestor of
420 Suillineae and Coniophora/Serpula clade.

421 **Supplemental Figure S3. Neighbour-joining (NJ) tree of the Cation Diffusion Facilitator**
422 **(CDF) family proteins from selected fungi.** Sequences were aligned by the MAFFT
423 algorithm. Bootstrap values (1000 replicates) are indicated and branch lengths are
424 proportional to phylogenetic distances. Localization and substrate (metal) are indicated for
425 functionally characterized proteins. *S. luteus* sequences are framed. Zn clusters are collapsed.
426 V = vacuole; ER = endoplasmic reticulum, G = Golgi apparatus.

427 **Supplemental Figure S4. Heterologous expression of *SlZnT1* and *SlZnT2* in yeast**
428 **mutants.** Cultures of wild type and mutant yeast were tenfold serial diluted and spotted on
429 control and metal-supplemented SD medium. The wild type strain was transformed with the

430 empty vector, the mutant strains with either the empty vector or the vector containing *SIznT1*
431 or *SIznT2*. (a) A Co sensitive mutant $\Delta cot1$, (b) a Cd sensitive mutant Δycf and (c) a Mn
432 sensitive strain $\Delta pmr1$ were used. The experiment was carried out twice for three independent
433 clones and pictures were taken after 4 days of growth.

434 **Supplemental Figure S5. PCR-product separated on gel-red stained 0.8% agarose gel.**

435 (a) PCR using *SIznT2* targeting primers was run on cDNA samples of transformed yeast cells
436 and plasmid DNA (positive control). *SIznT2* transcript was detected in $\Delta zrc1$ yeast cells
437 transformed with *SIznT2* containing plasmid but not in cells transformed with the empty
438 vector (EV). (b) A PCR using primers targeting the plasmid was performed to control for
439 plasmid contamination of RNA samples. A PCR-product was detected for the plasmid DNA
440 sample only. The PCRs were carried out for three independent clones.

441 **Supplemental Figure S6. Zn concentration in transformed yeast cells in control**
442 **conditions or after exposure to Zn.** The wild type strain was transformed with the empty
443 vector, the mutant strain with either the empty vector or the vector containing *SIznT1* or
444 *SIznT2*. Data are the average +/- SE of three biological replicates, significant differences ($p <$
445 0.01; two-way ANOVA followed by Student-Newman-Keuls) are indicated by different
446 letters.

447 **Supplemental Figure S7. Fe and Mn concentration in transformed yeast cells in control**
448 **conditions or after exposure to Zn.** The wild type strain was transformed with the empty
449 vector, the mutant strain with either the empty vector or the vector containing *SIznT1* or
450 *SIznT2*. Data are the average +/- SE of three biological replicates, significant differences ($p <$
451 0.01; two-way ANOVA followed by Student-Newman-Keuls) are indicated by different
452 letters.

1 **Experimental procedures**

2 **Fungal material and growth conditions**

3 The isolate UH-Slu-P4 from a *Suillus luteus* basidiocarp collected in a pine plantation in Paal,
4 Belgium was used. Mycelium was cultured for one week on cellophane-covered solid Fries
5 medium (28 mM glucose, 5.4 mM ammonium tartrate, 1.5 mM KH_2PO_4 , 0.4 mM $\text{MgSO}_4 \cdot 7\text{H}_2\text{O}$,
6 5 μM $\text{CuSO}_4 \cdot 5\text{H}_2\text{O}$, 20 μM $\text{ZnSO}_4 \cdot 7\text{H}_2\text{O}$, 0.1 μM biotin, 0.5 μM pyridoxine, 0.3 μM riboflavin,
7 0.8 μM nicotinamide, 0.7 μM p-aminobenzoic acid, 0.3 μM thiamine, 0.2 μM Ca-pantothenate
8 and 0.8% agar; pH-adjusted to 4.8) as described by Colpaert *et al.* (2004). Fungal colonies were
9 used immediately in DNA and RNA extraction protocols or to prepare liquid cultures according
10 to Ruytinx *et al.* (2016). After one week, 1 g of spherical mycelia grown in liquid culture was
11 transferred to a petri dish containing 30 ml modified liquid Fries medium with a concentration of
12 0, 20, 200 or 1000 μM Zn and incubated shaking for 48h at 23°C. Zinc exposure was performed
13 in triplicate. Spherical mycelia (200 mg) were stored at -70°C for gene expression analyses or
14 used directly for staining of labile Zn pool.

15 **Localization of labile Zn pool in *S. luteus***

16 Spherical mycelia obtained from liquid cultures exposed to different concentrations of Zn (20,
17 200, 1000 μM) were mixed in fresh medium of the same composition and grown for two
18 additional days. Five mg FW mycelium was transferred to a 2 ml eppendorf tube with 1.5 ml
19 TBS (Tris Buffered Saline: 137 mM NaCl, 3 mM KCl, 25 mM Tris; pH 7) containing 5 μM
20 FluoZin3. Following an incubation of 30 min (shaking), mycelia were washed twice in TBS for 5
21 min. FluoZin3 fluorescence was visualized with a Zeiss LSM 510 META laser scanning confocal
22 microscope, using a Zeiss 40x NA1.3 oil immersion objective. The 488 nm excitation line of the
23 laser and a BP 500-550 nm emission filter were used. Image processing was carried out with
24 ImageJ (NIH, Bethesda, MD, USA) software.

25 **DNA extraction and genome walking**

26 Fungal material (100 mg fresh weight) was thoroughly ground in liquid nitrogen using a mortar
27 and pestle. DNA was extracted from the grounded tissue using the DNeasy Plant mini kit
28 (Qiagen). Concentration of the DNA was determined on a NanoDrop ND-1000
29 spectrophotometer and agarose gel analysis was used to control integrity. High quality DNA was
30 used in a genome walking protocol (Genome Walker kit, Clontech). Briefly, DNA was digested
31 by blunt end restriction enzymes, fragments were adaptor ligated and PCR was performed using
32 an adaptor primer and a gene specific primer. Degenerative primers (Supplementary table 1) were
33 designed based on 6 conservative domains of functionally characterized fungal Zn-CDF
34 transporters. Fifty µl reactions containing 10x Advantage 2 PCR Buffer, 0.2 mM dNTP mix, 0.2
35 µM adaptor and gene specific primer, 50x Advantage 2 Polymerase Mix (Clontech) and 1µl
36 fungal DNA were performed using touchdown cycling conditions (7 cycles of 25s at 94°C, 3 min
37 at 70°C; 32 cycles of 25s at 94°C, 3 min at 67°C and 1 cycle of 7 min at 67°C). Amplicons were
38 visualised on a 1.5% agarose/gelred (Molecular Probes) gel, excised and resolved using the
39 QIAquick Gel Extraction kit (Qiagen). Finally, PCR products were cloned into the pCR4-TOPO
40 vector (Invitrogen) and sequenced. Sequences were assembled using the Staden Package v1.6.0.
41 (www.Staden.SourceForge.net). New gene specific primers (Supplementary table 2) were
42 designed and the protocol was repeated until the whole gene sequence was obtained.

43 **RNA isolation, cDNA synthesis and rapid amplification of cDNA ends**

44 Total RNA was extracted from in liquid nitrogen ground fungal colonies (200 mg) using the
45 RNeasy Plant Mini Kit (Qiagen). RNA quality was assessed using the Agilent-2100 Bioanalyser
46 and RNA 6000 NanoChips (Agilent Technologies). Poly(A)⁺ RNA was isolated from 250 µg
47 samples of total RNA using Oligotex columns (Qiagen). One µg poly(A)⁺ RNA was converted
48 into double stranded cDNA and adaptor ligated using the Marathon cDNA Amplification Kit

49 (Clontech) following the manufacturer's instructions. cDNA was diluted 50x in Tricine-EDTA
50 buffer. RACE PCR was performed in 50 µl reactions containing 10x Advantage 2 PCR Buffer,
51 0.2 mM dNTP mix, 0.2 µM adaptor and gene specific primer (Supplementary table 2), 50x
52 Advantage 2 Polymerase Mix (Clontech) and 5 µl diluted cDNA. PCR-products were visualised
53 on a 1.5% agarose/gelred (Molecular Probes) gel and excised from the gel. After isolation and
54 clean up of the PCR-products (QIAquick Gel Extraction kit; Qiagen), they were cloned into the
55 pCR4-TOPO vector (Invitrogen) and sequenced. Sequences were assembled and aligned to the
56 gDNA sequences to identify gene structure. *In silico* translations were performed and
57 transmembrane domains predicted by TMHMM. The identified protein sequences were called
58 ZnT1 and ZnT2. All bio-informatic analyses were performed using CLC Main workbench 6.7
59 and plug-ins unless stated otherwise.

60 **Phylogenetic tree construction and reconciliation**

61 BLASTx against NCBI nr protein sequences and JGI Agaricomycotina gene catalog proteins
62 (using MycoCosm; Grigoriev *et al.*, 2012) was performed using the identified proteins and the
63 CDF-family domain as a query. CDF-family proteins of *S. luteus* and selected Ascomycota and
64 Basidiomycota species were inventoried using the following criteria: protein length between 350-
65 700 amino acids, minimum 5 predicted transmembrane domains, presence of a CDF conserved
66 domain or signature sequence (Montanini *et al.*, 2007). The inventoried protein sequences were
67 aligned together with previously functionally characterized fungal CDF transporters. This
68 alignment was used for phylogenetic tree construction using the neighbour-joining (NJ) method.
69 Bootstrap tests were conducted using 1000 replicates and branch lengths are proportional to
70 phylogenetic distance. A species tree was build using ITS-sequences retrieved from the UNITE
71 database. Phylogenetic trees were built in MEGA v6.06; NOTUNG v2.8.1.7 was used to
72 reconcile both phylogenies.

73 **Cloning**

74 One μg total RNA was used in a Quantiscript Reverse Transcription reaction (Qiagen), which
75 includes a genomic DNA elimination step and makes use of random hexamer priming. Specific
76 primers were designed to amplify full-length coding sequences of *SlZnT1* (left:
77 attcactcaacactcagcactcg; right: aacgcctgagacgggcgga) and *SlZnT2* (left: gtgccaaccacaatggcat;
78 right: tagtatcacagtggtcgg). PCR reactions were performed in a total volume of 25 μl , containing
79 10x High Fidelity PCR buffer, 0.2 mM dNTP-mixture, 2 mM MgSO_4 , 0.2 μM specific forward
80 and reverse primer, 1 μl cDNA and 0.5 U Platinum Taq High Fidelity DNA polymerase
81 (Invitrogen) using general cycling conditions (2 min at 95°C, 35 cycles of 30s at 95°C, 30s at
82 60°C, 1 min at 68°C, 1 cycle of 2 min at 68°C). Amplicons were purified using QIAquick PCR
83 purification Kit (Qiagen) according to manufactures instructions. Purified PCR-products were
84 cloned into the gateway entry vector pCR8/GW/TOPO (Invitrogen) and subsequently
85 transferred by LR-clonase (Invitrogen) to pYES-DEST52 (Invitrogen), pAG306GAL-ccdB-
86 EGFP or pAG306GAL-EGFP-ccdB (Alberti *et al.*, 2007) for complementation, Zn content
87 analysis and localisation by GFP fluorescence in yeast. Finally, the insert was sequenced in both
88 directions to assure correct fusion.

89 **Yeast mutant complementation**

90 The yeast strains used for heterologous expression of *SlZnT1* and *SlZnT2* are BY4741 (MAT a;
91 his3 Δ 1; leu2 Δ ; met15 Δ 0; ura3 Δ 0), Δzrc1 (BY4741; MAT a; his3 Δ 1; leu2 Δ ; met15 Δ 0; ura3 Δ 0;
92 YMR243c::kanMX4), Δcot1 (BY4741; Mat a; his3 Δ 1; leu2 Δ ; met15 Δ 0; ura3 Δ 0;
93 YOR316c::kanMX4), Δycf1 (BY4741; Mat a; his3 Δ 1; leu2 Δ ; met15 Δ 0; ura3 Δ 0;
94 YDR135c::kanMX4) and Δpmr1 (BY4741; Mat a; his3 Δ 1; leu2 Δ ; met15 Δ 0; ura3 Δ 0;
95 YGL167c::kanMX4) obtained from Euroscarf ([http://www.uni-](http://www.uni-frankfurt.de/fb15/mikro/euroscarf)
96 [frankfurt.de/fb15/mikro/euroscarf](http://www.uni-frankfurt.de/fb15/mikro/euroscarf)). Yeast cells were transformed according to the LiAc/PEG

97 method described by Gietz & Woods (2002). After transformation, cells were grown at 30°C in
98 synthetic defined (SD) medium without amino acids, containing 2% (w/v) glucose or galactose
99 (induction medium), supplemented with yeast synthetic dropout without uracil, (pH5.3). Positive
100 colonies were PCR tested to confirm transformation. For metal tolerance assays, yeast was grown
101 on induction medium to an OD_{600nm} of one to perform tenfold dilution series. The drop assays
102 were performed for three independent clones on control SD plates (2% w/v galactose) and SD
103 plates supplemented with 8 mM Zn; 30 µM Cd; 1 mM Co or 1 mM Mn. RNA was extracted
104 from colonies growing on control plates and converted in cDNA to verify transcription of the
105 transgene by PCR.

106 **Localisation by confocal imaging**

107 Yeast cells were transformed, expression was induced by galactose and functionality of the gene
108 product was tested as described previously (see yeast mutant complementation). Cells were
109 grown to an OD_{600nm} of one, vacuolar membranes were selectively stained with the red
110 fluorescence probe FM4-64 (Molecular Probes, Invitrogen) following Vida & Emr (1995). A 3 µl
111 droplet of yeast cells was analyzed at 20°C with a Zeiss LSM 510 META laser scanning confocal
112 microscope, using a Zeiss 63x NA1.4 oil immersion objective and 10x scanning zoom at
113 512x512 pixel resolution (image size: 8 bit, 14,62 µm²). For EGFP fluorescence analysis we used
114 the 488 nm excitation line of the laser and a BP 500-550 nm emission filter. For FM4-64
115 fluorescence analysis we used the 488 nm excitation line of the laser and a LP 560 nm emission
116 filter. Image processing was carried out with ImageJ (NIH, Bethesda, MD, USA) software.

117 **Zn content analysis of transformed yeast**

118 Yeast cells were transformed and expression was induced as described in “yeast mutant
119 complementation”. Wild type yeast containing the empty vector, Δ zrc1 yeast containing the
120 empty vector and Δ zrc1 yeast containing the *SIZnT1* or *SIZnT2* cDNA were grown in liquid SD

121 medium containing galactose and supplemented with different concentrations of Zn (0 μ M or 500
122 μ M). Zn treatments were performed for three independent clones. Yeast cells were harvested
123 when OD_{600nm} of the cultures equalled one. Cells were washed three times with 20 mM PbNO₃
124 and milli-Q water. After drying, cells were destructed in concentrated acid (HNO₃/HCl) and Zn
125 content was determined by inductively coupled plasma optical emission spectrometry (ICP-OES).

126 **Gene expression analysis**

127 Total RNA extraction and cDNA synthesis occurred as described before. Real-time PCR was
128 carried out in 10 μ l reactions containing fast SYBR Green Master Mix (Applied Biosystems),
129 300 nM gene-specific forward (ZnT1L or ZnT2L; supplementary table 2) and reverse primer
130 (ZnT1R or ZnT2R; supplementary table 2) and 2.5 μ l diluted cDNA (fivefold dilution in 1/10
131 Tris-EDTA buffer). An ABI PRISM 7500 sequence detection system (Applied Biosystems) and
132 fast cycling conditions (20s at 95°C, 40 cycles of 3s at 95°C and 30s at 60°C) were used. After
133 cycling, a dissociation stage was added to assure specificity of amplification. Data were
134 expressed relative to the sample with the highest expression ($2^{-(Ct-Ctmax)}$) and normalised against
135 four reference genes. GR975621, AM085297, AM085168 and TUB1 were used as reference
136 genes according to Ruytinx *et al.* (2016). The normalisation factor for each sample was
137 calculated as the geometric mean of the relative expression of the four reference genes. The
138 significance of differences in expression level was examined by 2-way ANOVA and Tukey post-
139 test.

140 **References**

141 Alberti, S., Gitler, A.D., Lindquist, S. (2007) A suite of gateway cloning vectors for high-
142 throughput genetic analysis in *Saccharomyces cerevisiae*. *Yeast* 24(10): 913-919.

143 Colpaert, J.V., Muller, L.A.H., Lambaerts, M., Adriaensen, K., Vangronsveld, J. (2004)
144 Evolutionary adaptation to Zn toxicity in populations of Suilloid fungi. *New Phytol* 162:
145 546-559.

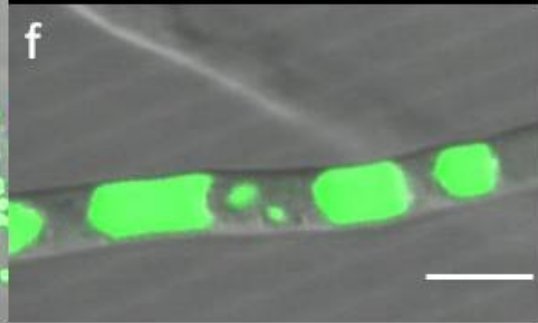
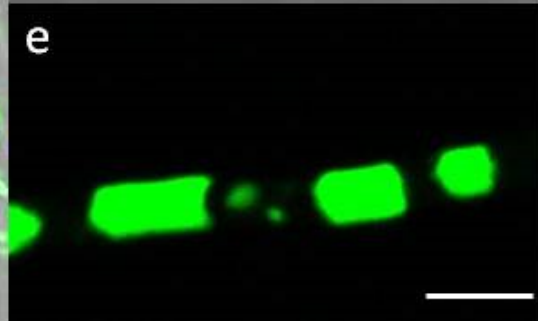
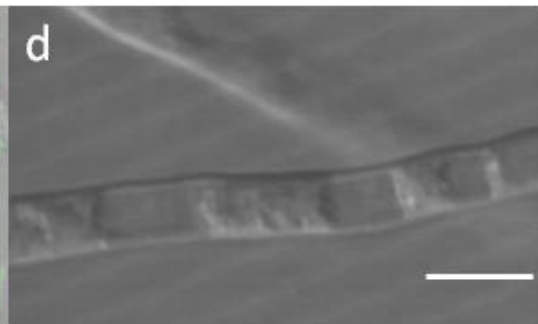
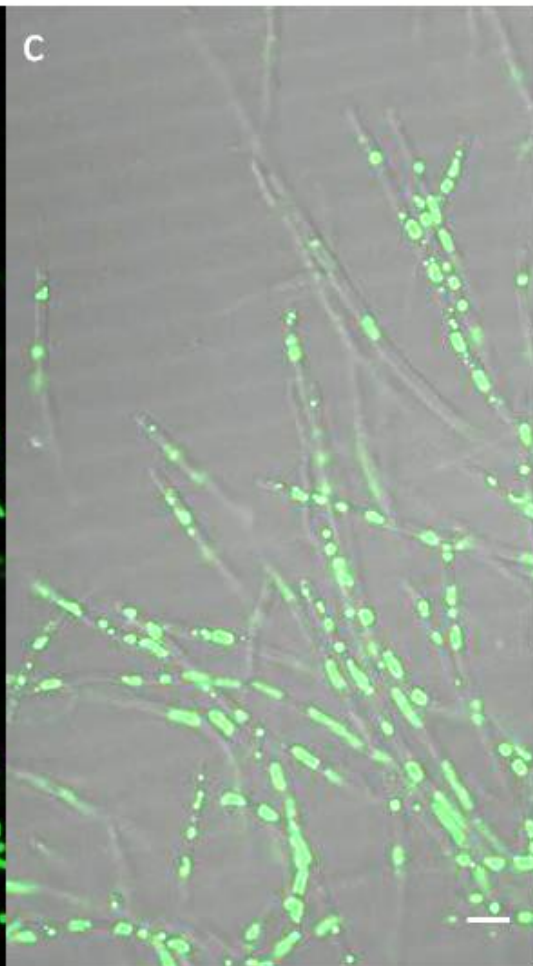
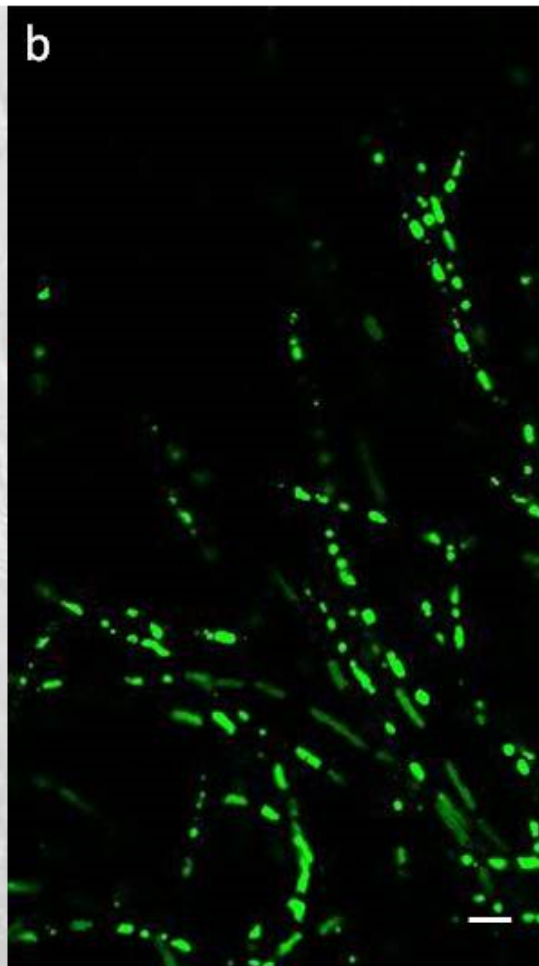
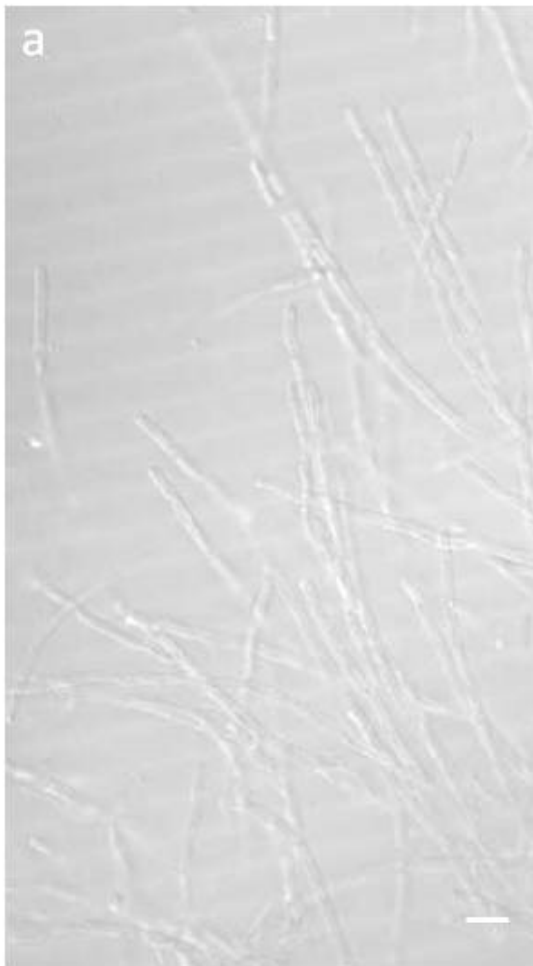
146 Gietz, D.R., Woods, R.A. (2002) Transformation of yeast by lithium acetate/single-stranded
147 carrier DNA/polyethylene glycol method. *Method Enzymol* 350: 87-96.

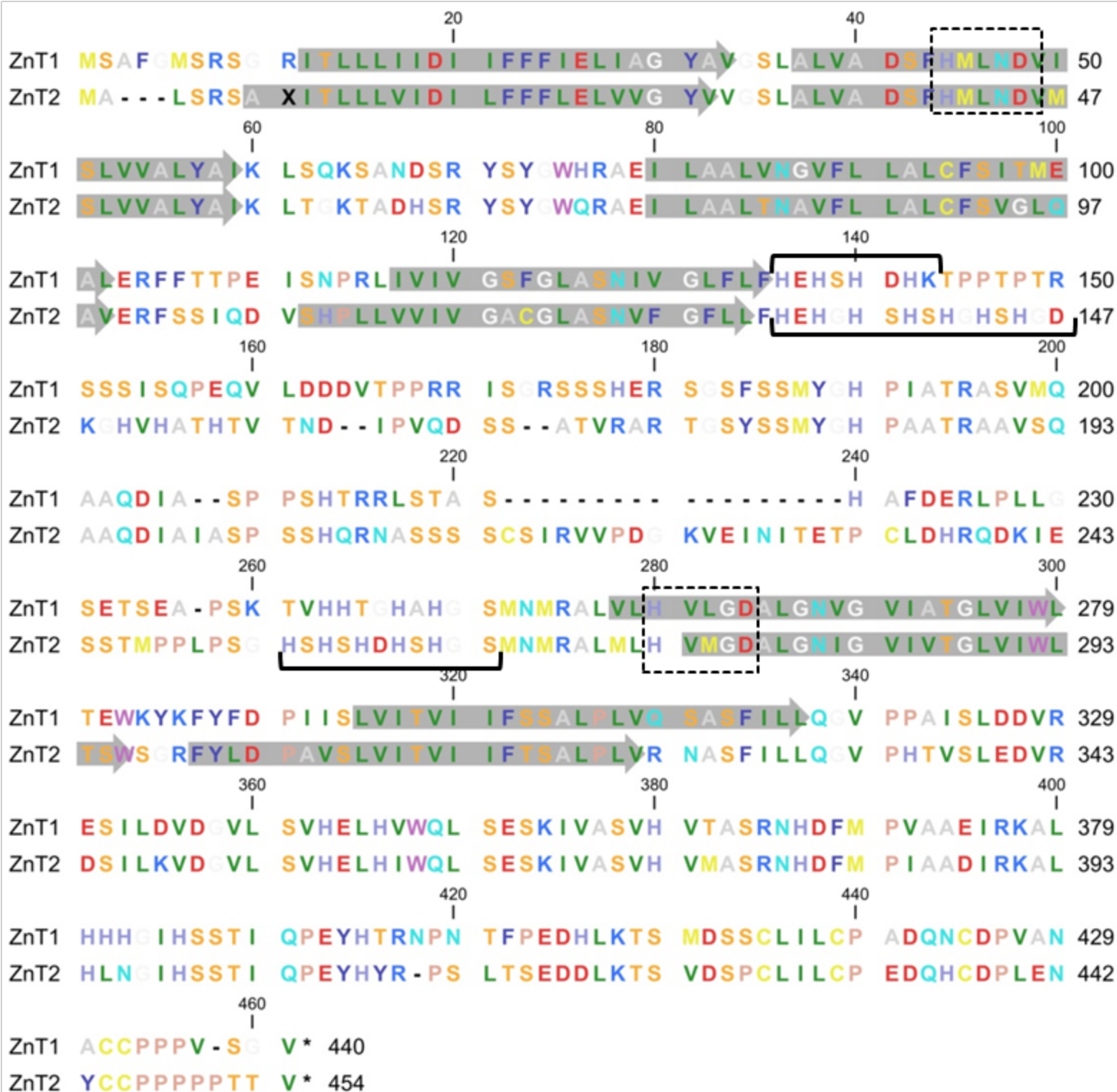
148 Grigoriev, I., Nordberg, H., Shabalov, I., Aerts, A., Cantor, M., Goodstein, D., Kuo, A.,
149 Minovitsky, S., Nikitin, R., Ohm, R. *et al.* 2012. The genome portal of the department of
150 energy joint genome institute. *Nucleic Acids Res* 40(D1): D26-D32.

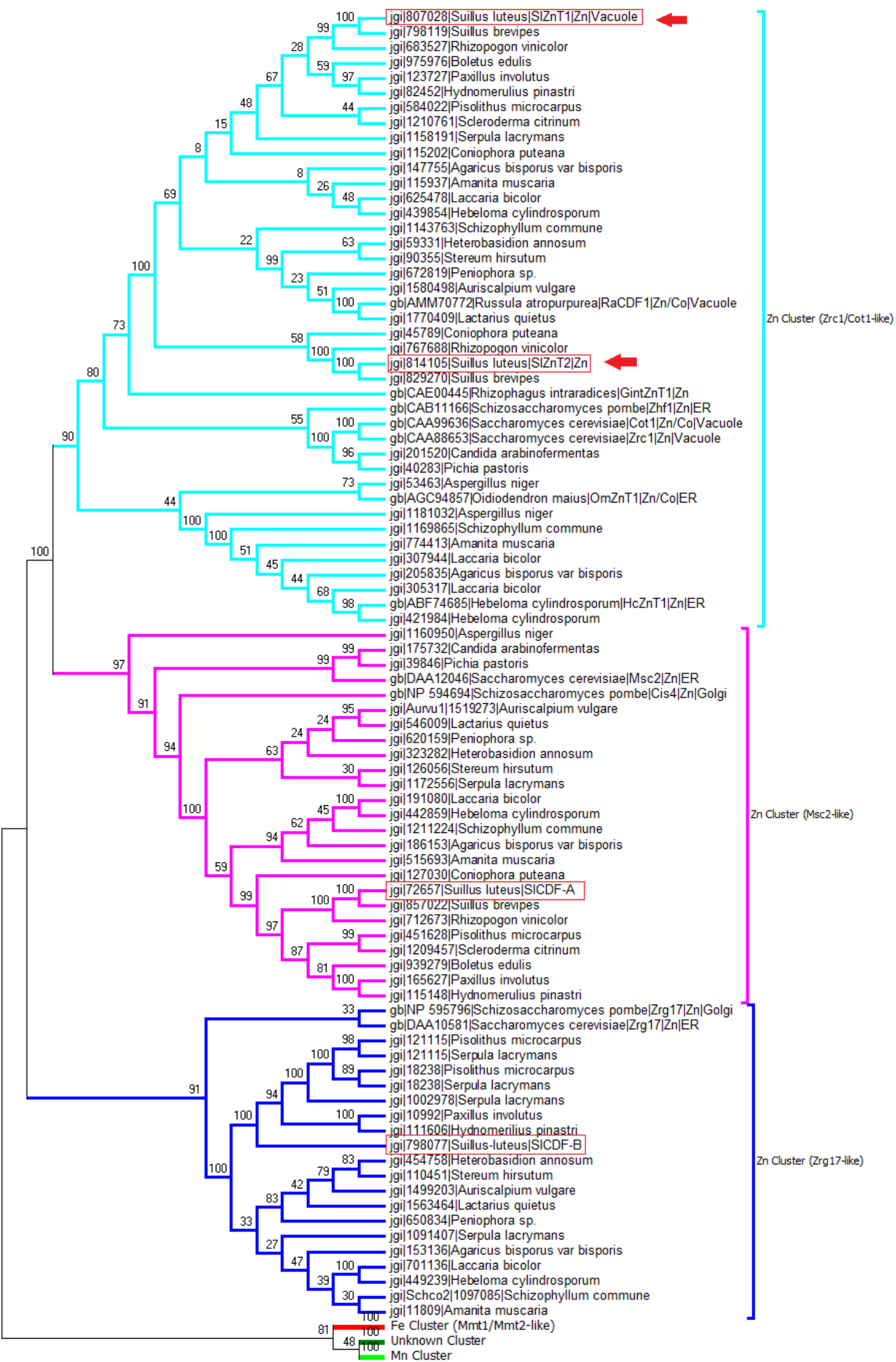
151 Montanini, B., Blaudez, D., Jeandroz, S., Sanders, D., Chalot, M. (2007) Phylogenetic and
152 functional analysis of the cation diffusion facilitator (CDF) family: improved signature
153 and prediction of substrate specificity. *BMC Genomic* 8: 107-122.

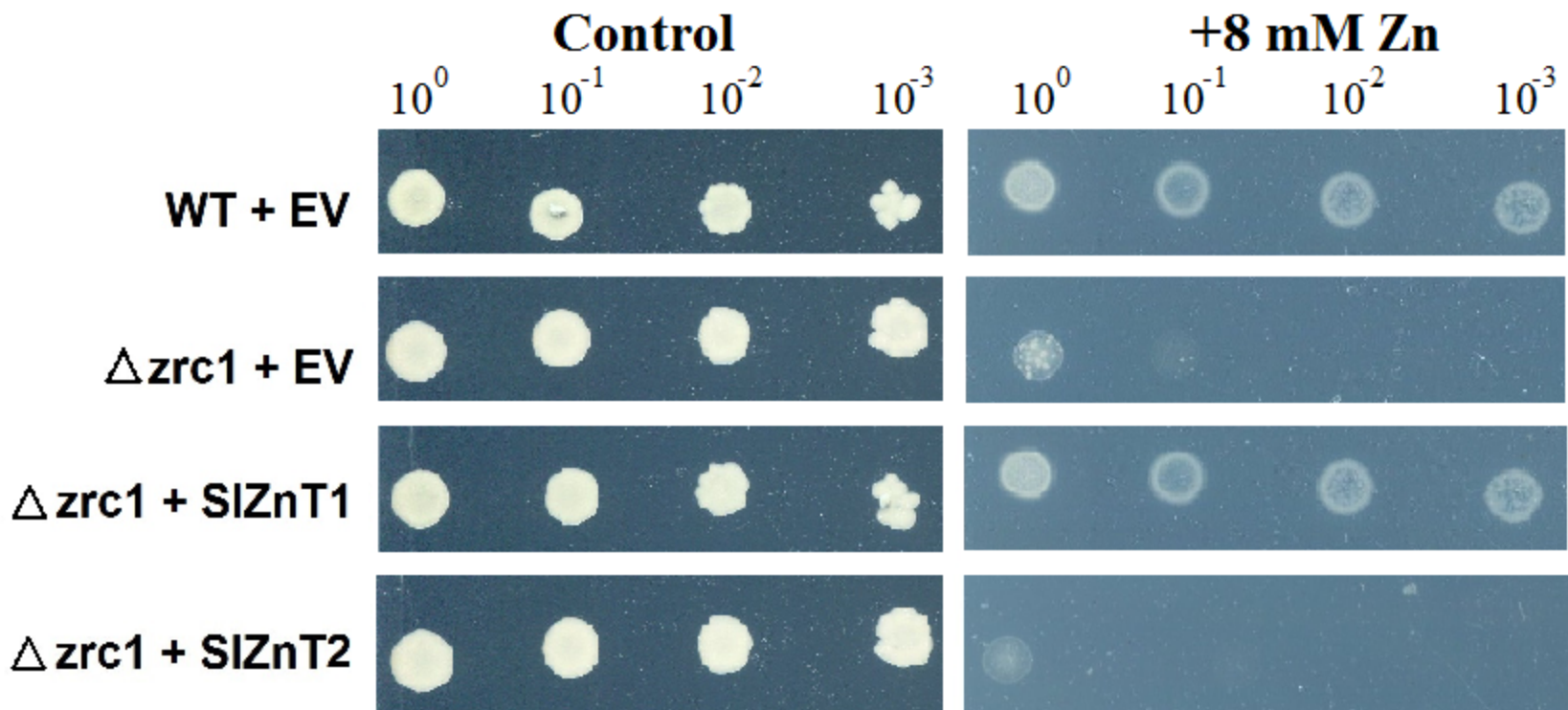
154 Ruytinx, J., Remans, T., Colpaert, J.V. (2016) Gene expression studies in different genotypes of
155 an ectomycorrhizal fungus require a high number of reliable reference genes. *Peer J*
156 *Preprints* 4: e2125v1.

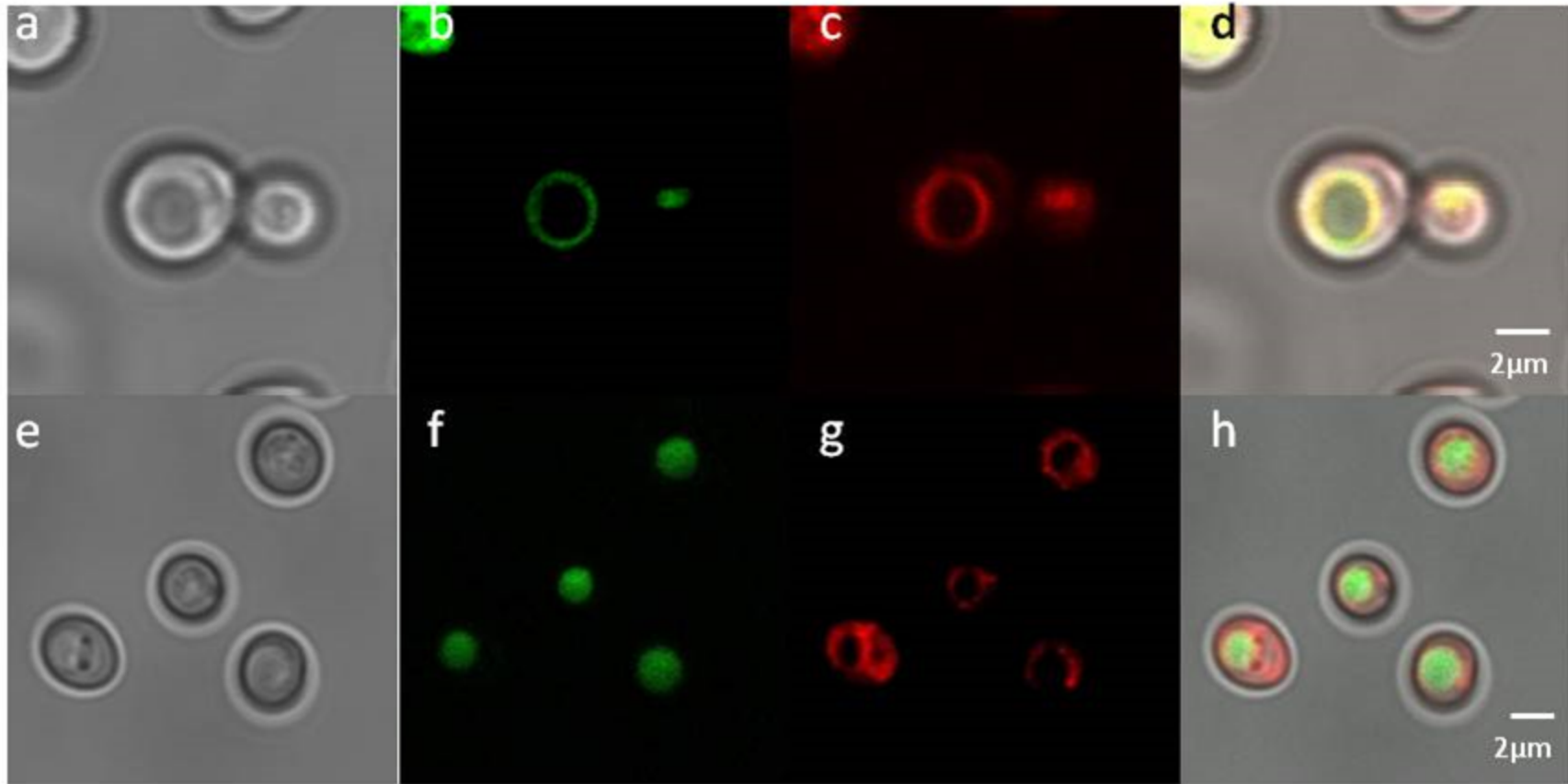
157 Vida, T.A., Emr, S.D. (1995) A new vital stain for visualizing vacuolar membrane dynamics and
158 endocytosis in yeast. *J Cell Biol* 128(5): 779-792.



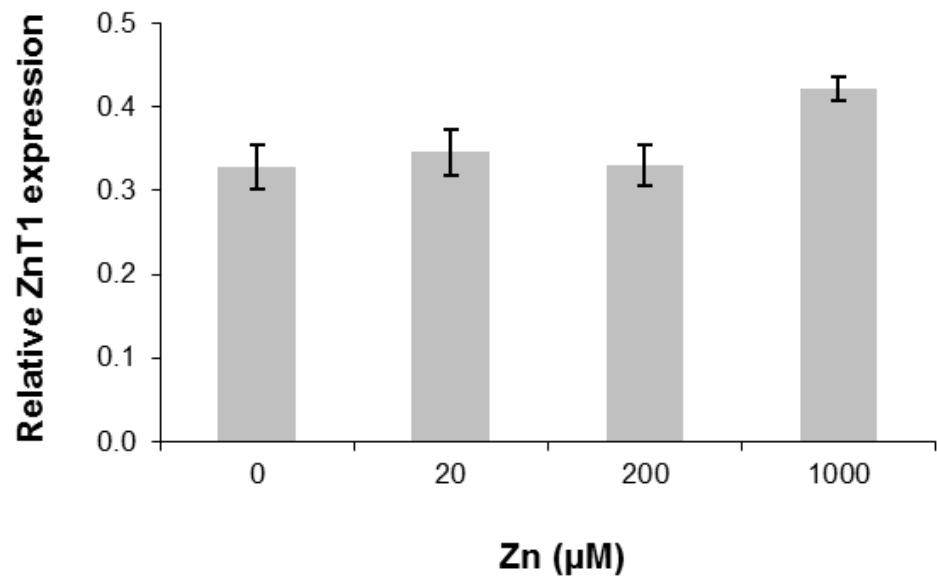




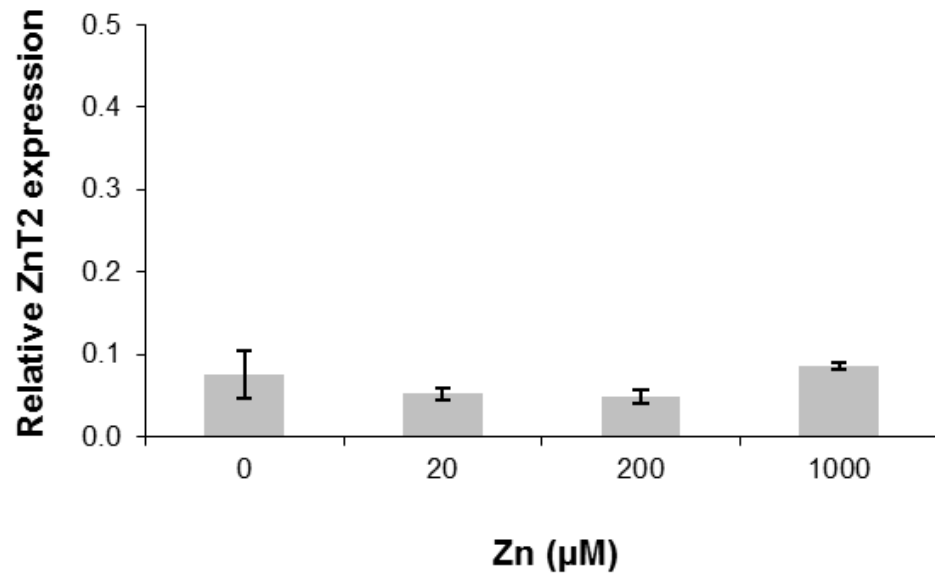




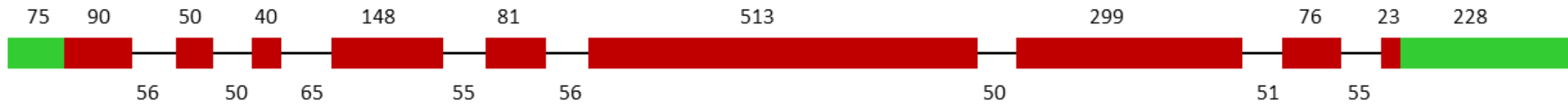
(a)



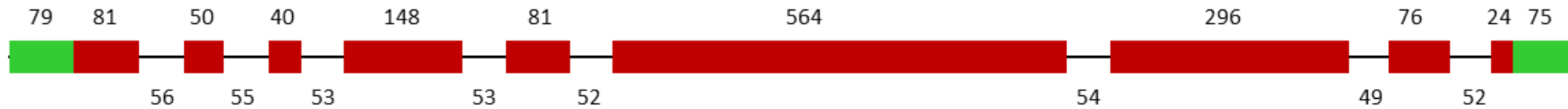
(b)

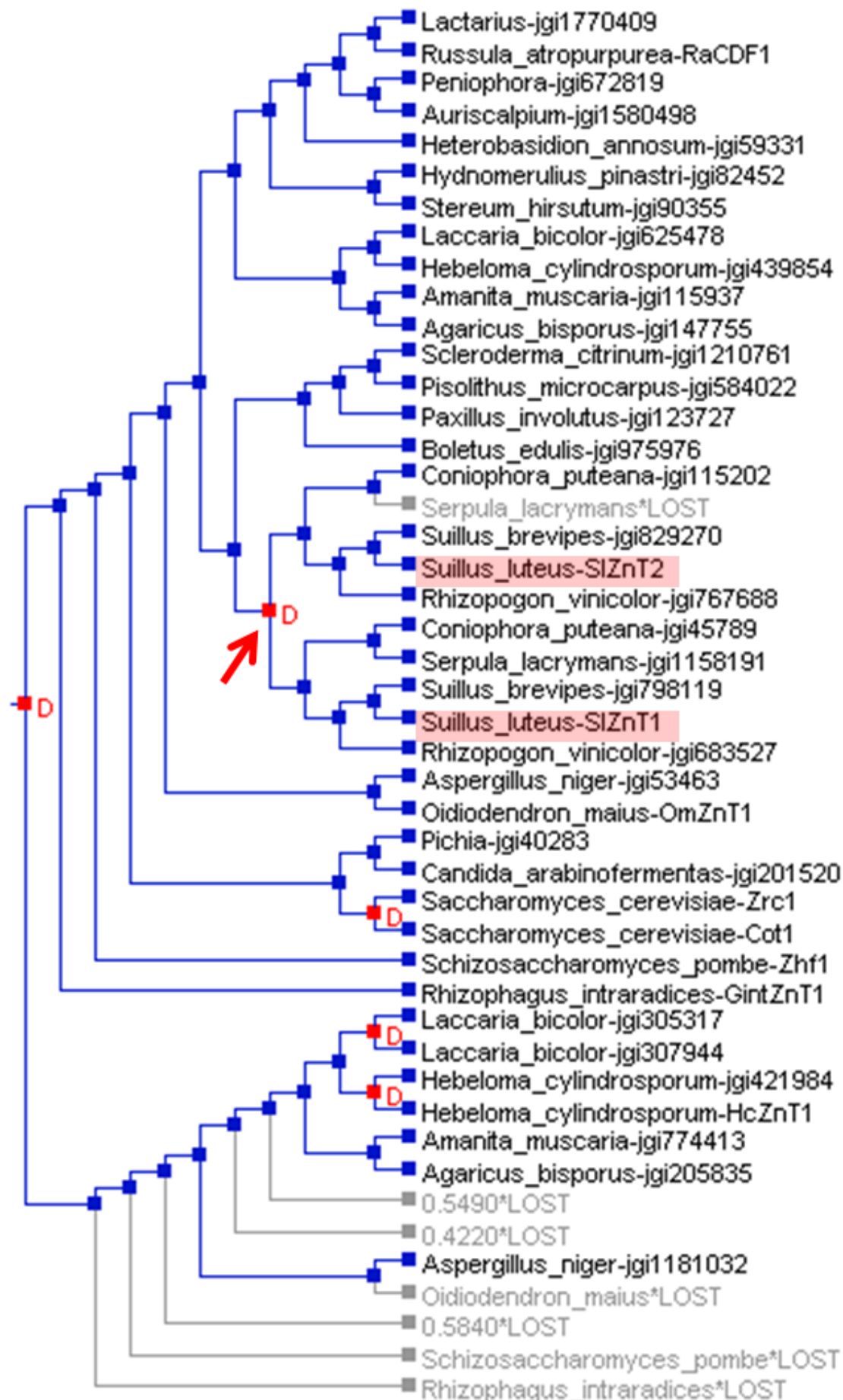


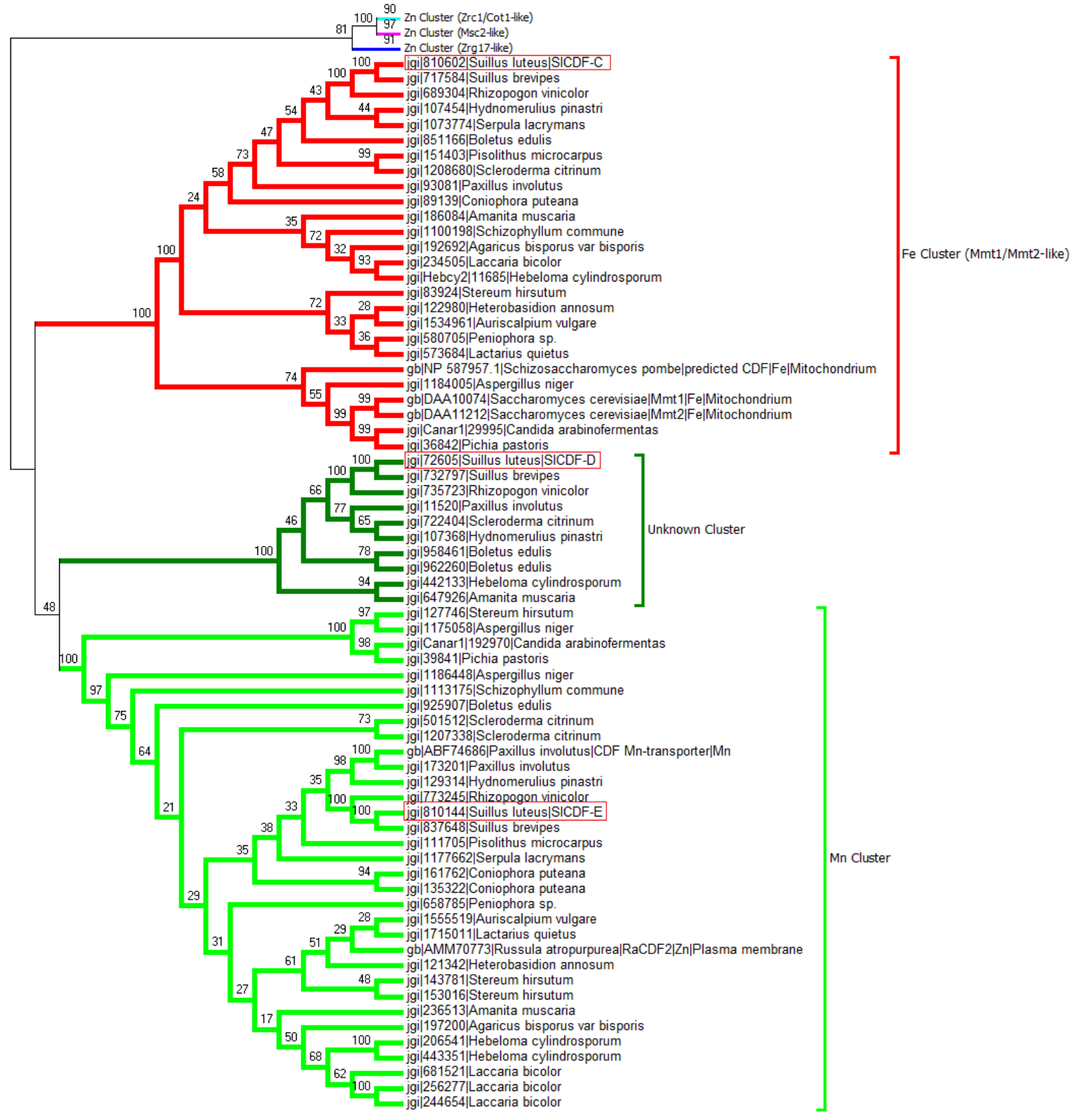
ZnT1

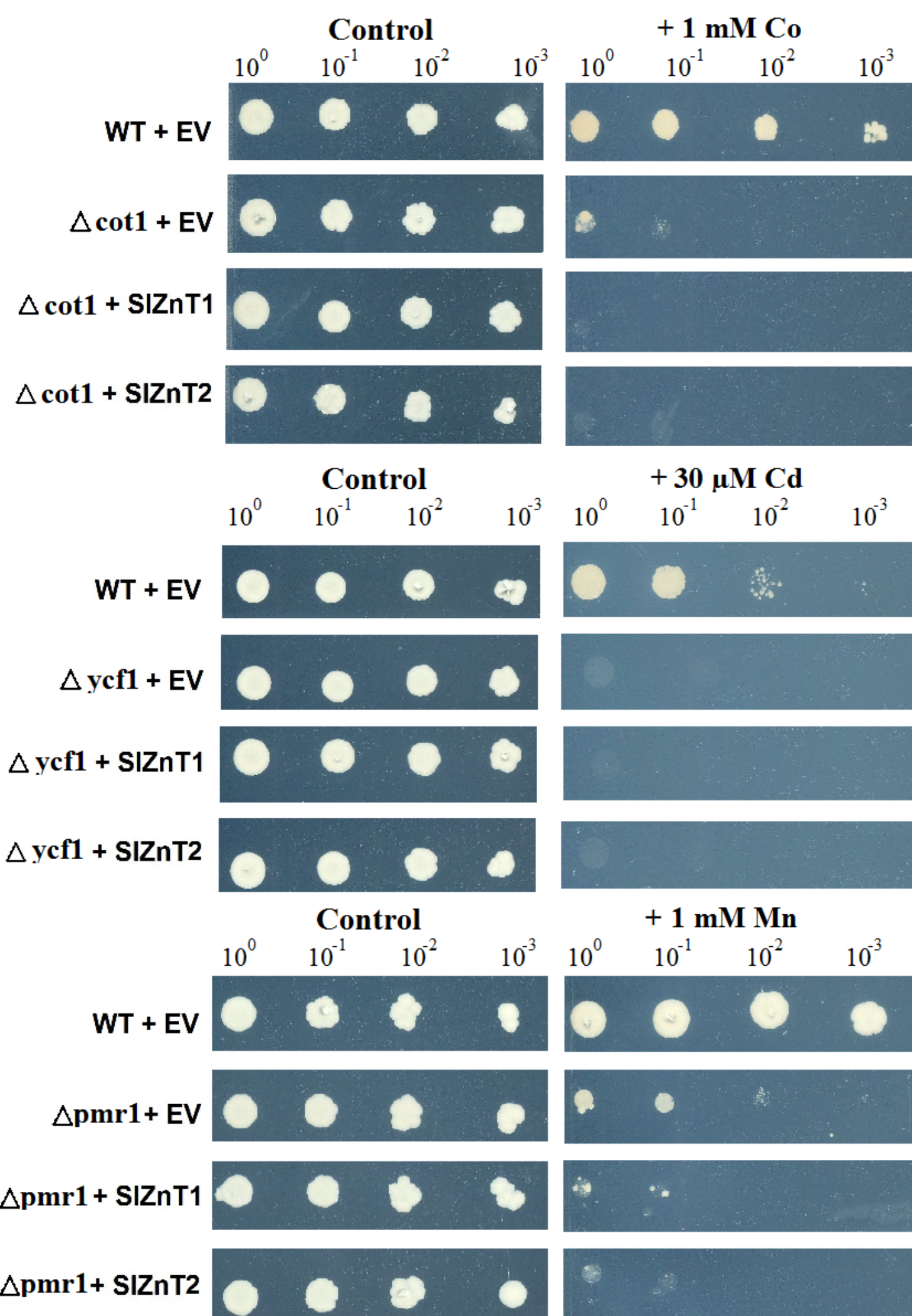


ZnT2

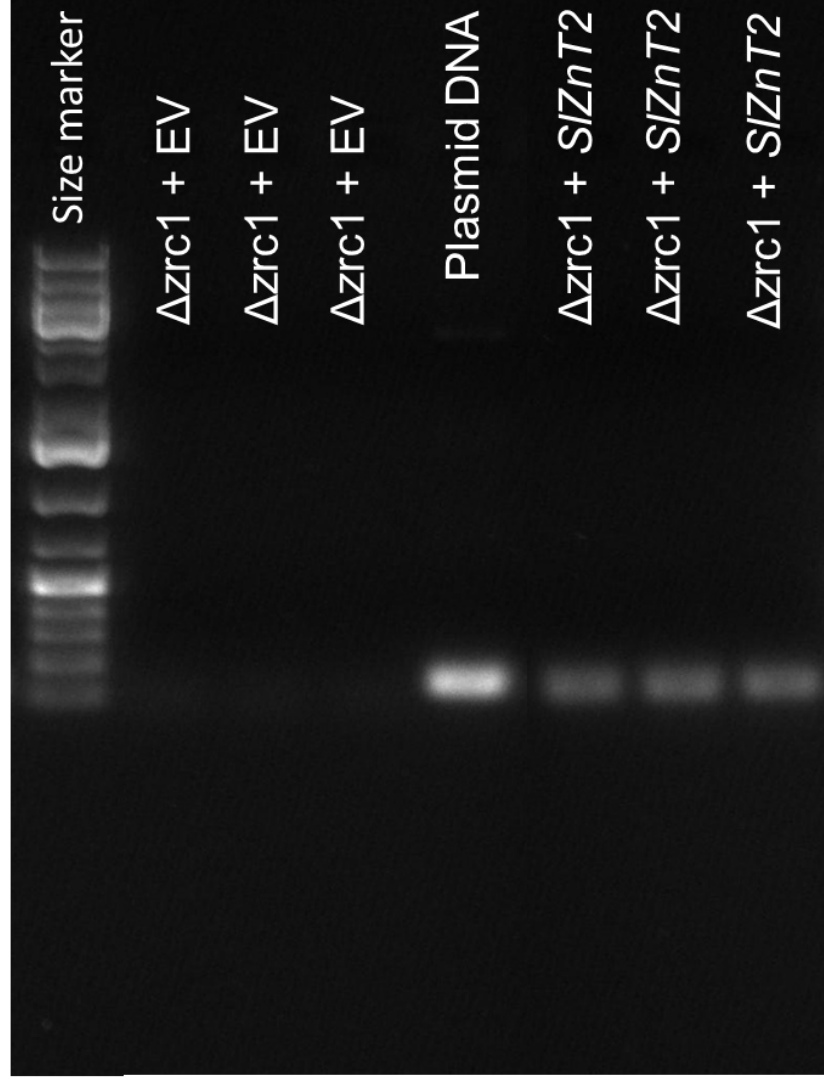








(a)



(b)

